

94-366



ОБЪЕДИНЕННЫЙ
ИНСТИТУТ
ЯДЕРНЫХ
ИССЛЕДОВАНИЙ
ДУБНА

E14-94-366

A.Yu.Didyk, W.R.Fahrner¹, Th.Fries², M.S.Rusetskii³,
V.S.Varichenko³, A.M.Zaitsev³

SURFACE MODIFICATION OF DIAMOND
IRRADIATED WITH SWIFT HEAVY IONS

Submitted to «Nuclear Tracks Radiation Measurements»

¹University of Hagen, 58084 Hagen, Germany

²Gunther Systemtechnik GmbH, D-53639 Königswinter, Germany

³University of Minsk, 220060 Minsk, Belarus

1994

1. INTRODUCTION

Recently it was predicted that tracks of heavy ions with energies of MeV/amu have relatively small lateral size in diamond [1], actually in the range of about a few nanometers. A model of ion tracks in superhard semiconductors has been proposed in [2]. In the schematic view the ion tracks are presented as rod-like macrodefects. According to this model the central core of a track consists of a significantly lower atom density compared with regular crystal matrix (in diamond this lack of density may have a value of up to 20%).

Ion tracks are specific defects of solids caused by high energy ion irradiation. The track formation mechanism and the parameters of the formed tracks are strongly controlled by the intensity of electronic stopping power of the fast ions in solids and by the characteristic properties of the irradiated materials.

The appearance of ion tracks has been unambiguously established in many insulating materials by different methods [3,4], including direct observation with high resolution electron microscopy [5]. The existence of ion tracks in superhard semiconductors has been shown by now only with indirect methods like luminescence or electron spin resonance (ESR) [6,7]. For further investigations it appears to be indispensable to prove the obtained data with direct methods. From this point of view the most interesting method is the scanning tunneling microscopy (STM). Firstly, the scanning tunneling microscopy gives opportunity to observe and investigate individual ion tracks on the irradiated surface with nm-scale resolution. Secondly, with this unique method it is possible to control individual ion tracks for potentiostatic measurements.

2. EXPERIMENTAL

High pressure, high temperature synthetic boron doped diamonds were used for the investigations. The boron impurity in the crystals during growth from boron containing media was 0.5% of boron. This results in a specific resistance of about $3 \Omega \cdot \text{cm}$. High energy irradiation of the samples by ^{84}Kr ions with an energy of 210 MeV and an ion fluence in the range of $Ft=10^{12}$ ions/cm² was carried out exposing a [111] as-grown

surface of a synthetic diamond crystal at the cyclotron U-400. The samples of natural diamonds were irradiated by ^{40}Ar (25 MeV) and ^{129}Xe (124 MeV) ions at the cyclotron U-300.

The samples have been investigated by the STM and SEM before and after irradiation with the high energy ions characterizing always the same macroscopic region of the surface. For the STM measurements, no further treatment of the samples was necessary.

The SEM investigations were carried out with the use of scanning electronic microscope JSM-840. The resolution of this microscope is 40 Angstrom. The STM used for the investigations is a homebuilt digitally controlled system equipped with a large scan option for imaging surface areas up to $22\ \mu\text{m} \times 22\ \mu\text{m}$ [8,9]. The experiment is run at ambient pressure using mechanically prepared tips from thin Pt/Ir - wires. Atomic resolution of pyrolytic graphite (HOPG) was obtained probing the imaging conditions of the tips. Scan ranges from $1\ \text{nm} \times 1\ \text{nm}$ up to $22\ \mu\text{m} \times 22\ \mu\text{m}$ were used, registering only images reproducible for multiple scans of the same surface region. The bias voltage was about - 2.5 V at the sample and the tunneling current was 1.0 nA for all measurements. Imaging conditions for semiconductor surfaces investigated at ambient pressure have been tested with elemental and CVD-diamond films. The scanning speed used was in the range of about 500 nm/second to avoid charging effects at the surface. The evolution of the experiments included topographs as well as profiles and rms-roughness data of the surfaces.

3. RESULTS AND DISCUSSION

At the beginning the amorphization of the semiconductor single crystals irradiated by different heavy ions was studied with the use of the back scattering technique (BST) [10,11]. The effect of low level amorphization of single crystals irradiated by the heavy ions with the high level of inelastic losses of energy was obtained. The same result was observed under the investigation of diamond single crystal, too [11]. For the understanding of this phenomenon we began the investigation of the diamond surface irradiated by different heavy ions.

The surface of diamond irradiated by ^{129}Xe and ^{40}Ar ions was investigated with the use of SEM technique. The energies of these ions are 124 MeV and 25 MeV. In fig.1 it is possible to see the surfaces of the natural diamond before (a) and after (b) irradiation by ^{129}Xe ions. The fluence was $F_t = 5 \times 10^{15}\ \text{ion/cm}^2$. One can see that before the irradiation the diamond surface was a smooth one, but after the irradiation there are smooth and rough regions of the surface. The picture of the diamond surface after irradiation by ^{40}Ar ions differed in comparison with ^{129}Xe irradiation. It is clear from fig.1.c. In this case the ion fluence was $F_t = 8 \times 10^{15}\ \text{ion/cm}^2$ and the structure of surface was totally amorphized (the swelled type of the surface). In the case of ^{129}Xe ions the diamond conserved the crystalline structure, but in the case of ^{40}Ar ions the crystal was totally amorphized. This result was obtained with the use of BST [11]. Such differences may be connected with the evaporation of small diamond particles under the irradiation and then their condensation on the surface. The inelastic losses of energy for ^{129}Xe (the energy is $E = 124\ \text{MeV}$, the projective range $R_p = 6.34\ \mu\text{m}$), ^{40}Ar ($E = 25\ \text{MeV}$, $R_p = 3.85\ \mu\text{m}$) ^{84}Kr ($E = 210\ \text{MeV}$, $R_p = 14.0\ \mu\text{m}$) near the surface are

$$\begin{aligned} (dE/dx)_{\text{inel}}^{\text{Xe}} &= 25\ \text{MeV}/\mu\text{m}, \\ (dE/dx)_{\text{inel}}^{\text{Kr}} &= 19\ \text{MeV}/\mu\text{m}, \\ (dE/dx)_{\text{inel}}^{\text{Ar}} &= 9\ \text{MeV}/\mu\text{m}. \end{aligned} \quad (1)$$

These results were obtained with the use of computer code TRIM-90. Really, it is possible to calculate the temperature in the ion track during the passage of a heavy ion with the use of the expression:

$$T = (dE/dx)_{\text{inel}} / \pi R_i^2 C_i \rho_i, \quad (2)$$

where the $(dE/dx)_{\text{inel}}$ is the inelastic losses of energy, R_i is the radius of the ion track, C_i and ρ_i are the density and the heat capacity of the diamond. At the beginning it is possible to estimate the ion track diameter like $R_{\text{Xe}} = 50\ \text{A}$. The parameters in the equation are $C_i = 1.92\ \text{J/g/grad}$ (for the temperatures higher than $T > 1320\ \text{K}$) and $\rho_i = 3.51\ \text{g/cm}^3$. The track radius of ^{40}Ar can be obtained from the equation [12]:

$$R_{Ar} = R_{Xe} \left[\frac{(dE/dx)_{inel}^{Ar}}{(dE/dx)_{inel}^{Xe}} \right]^{1/6} = 42 \text{ \AA}$$

$$R_{Kr} = R_{Xe} \left[\frac{(dE/dx)_{inel}^{Kr}}{(dE/dx)_{inel}^{Xe}} \right]^{1/6} = 47.6 \text{ \AA} \quad (3)$$

So, the temperatures in ion tracks of ^{129}Xe and ^{40}Ar are:

$$T_{Xe} \cong 7600 \text{ K}, \quad T_{Ar} \cong 3900 \text{ K} \text{ and } T_{Kr} \cong 6300 \text{ K}. \quad (4)$$

The melting temperature of diamond is $T_{mel} = 4300\text{K}$. One can make a conclusion that the temperature in the xenon ion track is higher than the melting temperature of the diamond, so the mechanism of the diamond particles evaporation can be realized in the cases of Xe and Kr ion irradiation in the difference of Ar ion irradiation.

The investigation of the diamond surface irradiated by heavy ions was carried out with the use of a high resolution STM method, because it is possible to determine the changes of the surface after passing of single ions when the ion tracks don't overlap.

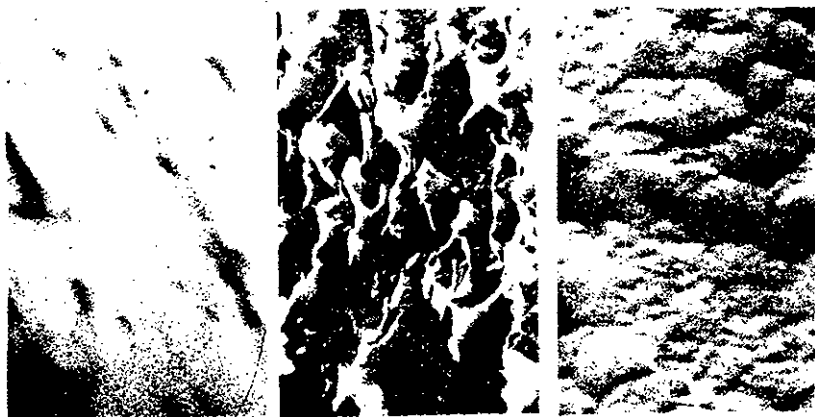


Fig.1. The SEM image of the the diamond surfaces before (a) and after irradiation by ^{124}Xe (b) (The ion fluence is $Ft = 5 \times 10^{15} \text{ ion/cm}^2$) and ^{40}Ar (c) ions (The ion fluence is $Ft = 8 \times 10^{15} \text{ ion/cm}^2$).

STM-images of non-irradiated and irradiated by ^{84}Kr surfaces are presented in fig.2. Fig.2a shows a surface of $3820 \text{ \AA} \times 2319 \text{ \AA}$ before treatment with the ion beam, the maximum height being 10.7 nm . The characteristic step shapes are shown on the flat surface, having a rms roughness of 0.2 nm . Fig.2b gives an example of the surface morphology after the irradiation. The scan range is $125 \text{ nm} \times 125 \text{ nm}$ with a maximum height of 1.5 nm . It is clearly seen that the ion irradiation results in a strong roughening of the surface. The irradiated surfaces appeared to have a lower conductivity compared to the untreated surfaces as probed by slightly different tunneling conditions. The lowering of conductivity is due to implantation effects. The profile of a characteristic region in fig.2b, that is given in fig.2c, proves that the roughness of the surface is actually caused by individual pits. The density of pits covering the irradiated surface equals roughly the irradiation fluence ($Ft \cong 10^{12} \text{ ion/cm}^2$). From this fact it is deduced that the pits are results of the ion impact onto the surface. The observed diameters of the pits start at about 3 nm rising locally to about 20 nm . From the diameter distribution of the pits and theoretical proposal of the ion track sizes we conclude, that the 3 nm pits are caused by single ions, while greater pits are representing multiple ion impact at the same position on the surface.

The ion track can be formed in a solid matrix by two mechanisms: thermal peak and coulomb explosion [13]. The thermal peak mechanism is effective in substances possessing thermal conductivity low enough to prevent rapid dissipation of the energy deposited along the ion path via electronic stopping. An estimation made in accordance with the model of the work in ref. [14] gives very low efficiency of the thermal mechanism in diamond because of its very high thermal conductivity.

In the difference of such estimations one can get the temperatures at the Xe and Kr ion tracks from the eq.(2) and $T_{Xe,Kr} > T_{mel}$ with the use of measured pit diameters ($D_{Xe} \cong 3 \text{ nm}$) and the lifetime τ_i of such ion track enough for the rapid evaporation process. Also we are sure it is not correct to describe so far non equilibrium state of diamond with the use of equilibrium parameters, like heat conductivity and so on.

In the process of material evaporation under the irradiation by electrons the critical density of power can be introduced:

$$W_{cr} = 4 \kappa_i L_{evap} \rho_i X_{pit} / D_{pit}^2 \quad (5)$$

where κ_i is the temperature conductivity. For diamond

$$\kappa_i = K_i / C_i \rho_i = (0.81 - 4.44) \text{ cm}^2 / \text{c} \quad (6)$$

here $K_i = 5.5 \text{ W/cm/K}$ (for ordinary type of diamond, $K_i = 10 \text{ W/cm/K}$ (for I type of diamond) and $K_i = 20-30 \text{ W/cm/K}$ (for II type of diamond), L_{evap} is the evaporation heat (for diamond $L_{evap} = 6 \times 10^4 \text{ J/g}$), X_{pit} and D_{pit} are the depth and diameter of track corresponding. For the measuring value of pit size ($D_{pit} = 3 \text{ nm}$) and with the estimation of the depth of pits like $X_{pit} \approx 3 \text{ nm}$ one can calculate the critical value of power density:

$$W_{cr} \approx (0.23 - 1.25) \times 10^{13} \text{ W/cm}^2 \quad (7)$$

The volume distribution of inelastic energy losses can be described in the following form:

$$\frac{d^3 E}{dx dR d\phi} = (dE/dx)_{inel} \times \text{EXP}(-R^2/R_c^2) / \pi R_c^2 \quad (8)$$

here R_c is the ion track radius.

So, the energy of heavy ion deposited into the volume:

$$V = \pi D_{pit}^2 X_{pit} / 4 \quad (9)$$

(for the calculations it is possible to estimate $X_{pit} \approx D_{pit}$) can be obtained from the equation:

$$\Delta E = \int_0^{2\pi} d\phi \int_0^{D_{pit}} dx \int_0^{R_{pit}} RdR \frac{d^3 E}{dx dR d\phi} \quad (10)$$

The density of ion power loss in the volume V can be calculated with the use of the expression:

$$W_{ion} = \frac{4\Delta E}{\pi D_{pit}^2 t_{fl}} \quad (11)$$

here the time of ion passing of the length X_{pit}

$$t_{fl} = X_{pit} / (2E_{ion}/M)^{1/2} \quad (12)$$

M and E are the mass and energy of ion respectively. After calculations with the use of the equations (8)-(10) we obtained the density of power for xenon ions:

$$\begin{aligned} W_{Xe} &\approx 6.61 \times 10^{13} \text{ W/cm}^2 \quad (R_{Xe} = 50 \text{ \AA}) \\ W_{Kr} &\approx 8.88 \times 10^{13} \text{ W/cm}^2 \quad (R_{Kr} = 47 \text{ \AA}) \end{aligned} \quad (13)$$

Comparing the (7) and (13), one can see that for the Xe and Kr ions $W_{Xe, Kr} \gg W_{cr}$. The calculation of the power density for ^{40}Ar ions gives the value $W_{Ar} \approx 1.9 \times 10^{13} \text{ W/cm}^2$ (for $R_{Ar} = 42 \text{ \AA}$ and with the same values of X_{pit} and R_{pit} like xenon ions). So in this case $W_{Ar} > W_{cr}$, too. But the estimation for argon ions is not correct because we don't know the experimental values of X_{pit} and R_{pit} .

For this reason in the case of xenon ion irradiation the processes of carbon atom evaporation must be in the difference of argon ion irradiation because two conditions are realized:

$$W_{Xe} \gg W_{cr}, T_{Xe} > T_{mel} \text{ and } W_{Kr} \gg W_{cr}, T_{Kr} > T_{mel} \quad (14)$$

The same criteria were introduced for the description of evaporation processes in stainless steel irradiated by heavy ions [15]. The effects of inelastic sputtering of solids by ions was described in ref. [16].

The coulomb explosion mechanism appears to be much more effective in superhard semiconductors. Diamond being a very good insulator is able to keep electrically charged species in the crystal for a relatively long time. This time is believed to be long enough to allow the ionized atoms appearing during electronic stopping of fast ions to be pushed apart.

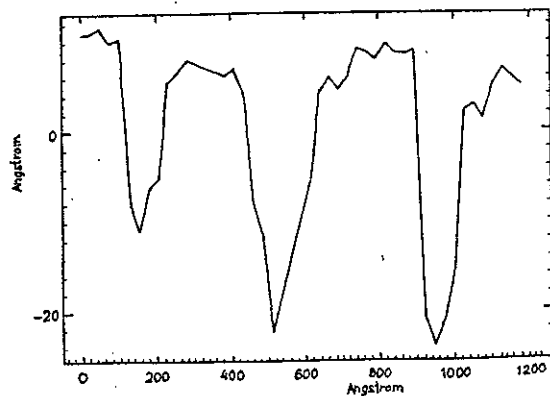
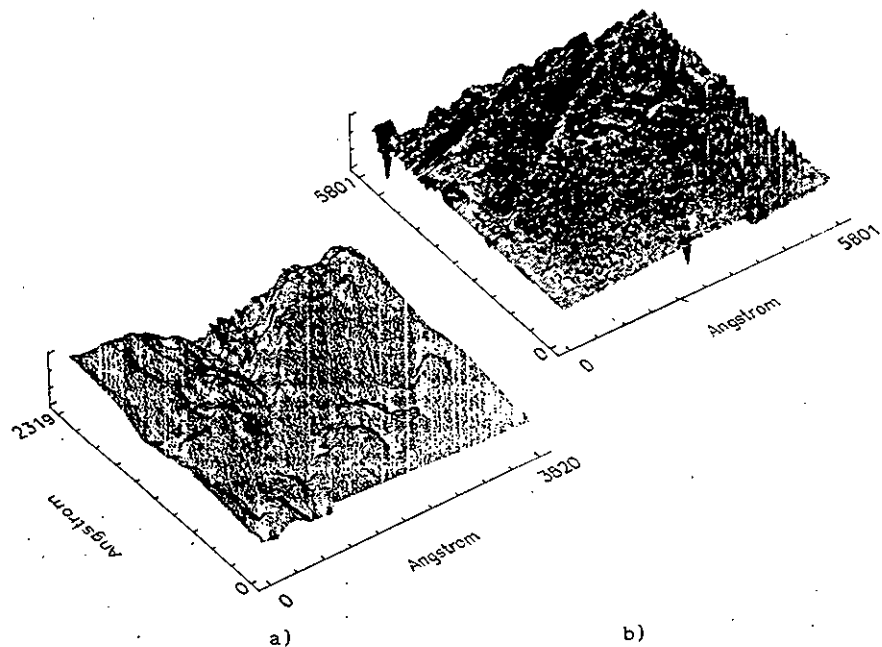


Fig.2. a) surface of boron doped synthetic diamond before irradiation, the scanning area is 3820 Å x 2319 Å, height is 10.7 nm.
 b) surface area of boron doped synthetic diamond after irradiation by heavy ions, 580 nm x 580 nm, height is 5.5 nm.
 c) characteristic profile showing individual ion tracks.

From our estimations we can introduce the model of individual track of heavy ions with the big value of inelastic losses of energy in irradiated diamond. In the schematic view of fig.3 the ion tracks are presented as rod-like microdefects^{17/}. The part of irradiated volume is evaporated and then condensated on the inhomogeneities on the surface. The central core of a track consists of the recrystallization volume (may be)^{10, 11/}. These processes are connected with the inelastic losses of ion energy. And on the big depth a track consists of the vacancies. This process is connected with the elastic losses of energy.

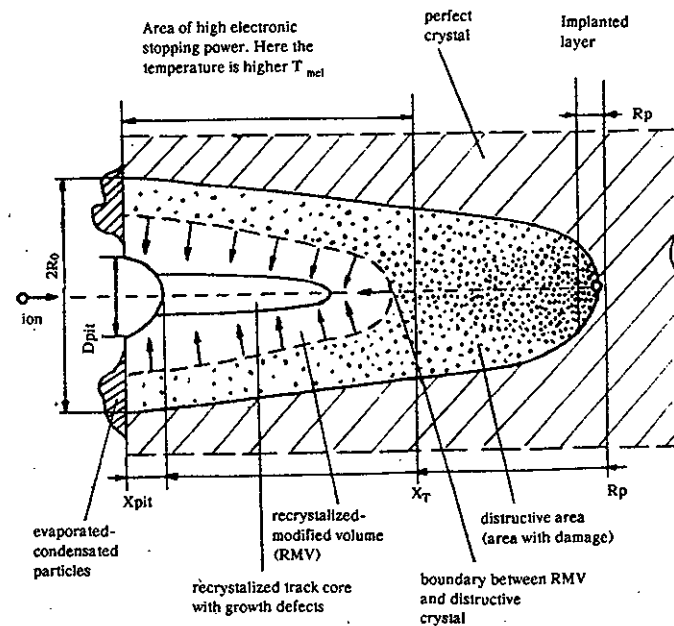


Fig.3. The scheme of tracks in solid matrix after irradiation by ions with energies over 1 MeV/amu.

REFERENCES

1. A. Yu. Didyk, V. S. Varichenko, A. M. Zaitsev, V. I. Kuznetsov, V. A. Skuratov, V. F. Stelmakh, V. D. Shestakov. JINR Commun. R14-86-411, Dubna (1986).
2. V. S. Varichenko, A. M. Zaitsev, A. A. Melnikov, V. F. Stelmakh. Sverhtverdye Materialy 1, p. 3-8 (1989) (in Russian).
3. F. Thibaudau, J. Coustry, E. Balanzat, S. Bouffard. Phys. Rev. Lett. 67, p. 1582-1585 (1991).
4. D. Albrecht, P. Armbruster, R. Spohr, M. Roth, K. Schaupt, H. Stuhmann. Appl. Phys. A37, p. 36-46 (1985).
5. J. M. Constantini, F. Ravel, F. Brisard, M. Caput, C. Cluzean. Nucl. Instrum. Meth. Phys. Res. B80/81, p. 1249-1254 (1993).
6. A. R. Filipp, V. V. Tkachev, V. S. Varichenko, A. M. Zaitsev, A. R. Chelyadinskii, Yu. A. Kluev. Diamond and Related Materials, 1, p. 791 (1989).
7. D. P. Erchak, V. G. Efimov, A. M. Zaitsev, V. F. Stelmakh, N. M. Penina, V. S. Varichenko, V. P. Tolstikh. Nucl. Instrum. Meth. Phys. Res. B69, p. 443-451 (1992).
8. Th. Fries, C. Becker, M. Bohmer, K. Wandelt. Fresenius J. Anal. Chem. 341, p. 193 (1991).
9. Th. Fries. Thesis, University of Bonn (1993).
10. S. A. Karamyan, Yu. Ts. Oganessian, V. N. Bugrov. Nucl. Instr. & Meth. B43, p. 153 (1989).
11. A. Yu. Didyk, A. M. Zaitsev, S. A. Karamian. JINR Rapid Commun. No. 4[37]-89, p. 44-49 (1989).
12. A. A. Davydov, A. I. Kalinichenko. Voprosu Atomnoi Nauki i Tekniki 3[36], p. 27-29 (1985) (In Russian).
13. R. L. Fleicher, P. B. Price, R. M. Walker. In.: Nuclear Tracks in Solids, University of California Press, Berkeley (1975).
14. L. E. Seiberling, J. E. Griffith, T. A. Tombrello. Rad. Eff. 52, p. 201-210 (1980).
15. A. Yu. Didyk. JINR Commun., R14-94-333, Dubna, p. 13 (1994).
16. I. A. Baranov, Yu. V. Martynenko, S. O. Tsepelevich and Yu. N. Yavlinskii. Usp. Fiz. Nauk, v. 156, p. 477-511.
17. A. Yu. Didyk. JINR Commun., R14-94-365, Dubna, p. 14 (1994).

Received by Publishing Department
on September 13, 1994.